Article

Feasibility Study of Cable Routing for Bi-Planar Trajectory Tracking in Cable Driven Lower Limb Exoskeleton

Rajan Prasad[1], Marwan El-Rich[1,2*], Mohammad I. Awad[2,3,4], Sunil K. Agrawal[5], Kinda Khalaf[2,3]

1 Department of Mechanical Engineering, Khalifa University of Science Technology & Research, Abu Dhabi, UAE; (rajanprasad460@hotmail.com , marwan.elrich@ku.ac.ae)
2 Health Engineering Innovation Center, Khalifa University of Science Technology & Research, Abu Dhabi, UAE
3 Department of Biomedical Engineering, Khalifa University of Science Technology & Research, Abu Dhabi, UAE; kinda.khalaf@ku.ac.ae
4 Khalifa University Center for Autonomous Robotic Systems (KUCARS), Khalifa University of Science Technology & Research, Abu Dhabi, UAE; mohammad.awad@ku.ac.ae
5 Department of Mechanical Engineering and Rehabilitation and Regenerative Medicine, Columbia University, New York, USA; sunil.agrawal@columbia.edu
* Correspondence: , marwan.elrich@ku.ac.ae ; +971 2 312 4193

Abstract: Although Cable driven rehabilitation devices (CDRD) have advantages over traditional link-driven devices, including lightweight, ease of reconfiguration, remote actuation, etc, the majority of existing lower-limb CDRD is limited to rehabilitation in the sagittal plane. In this work, we extend our previous sagittal plane model (2DOF) to accommodate hip motion in the frontal plane (abduction/adduction) toward studying the feasibility of tracking bi-planar motion (combined frontal and sagittal plane motion) via intra-planar cable routing. Two optimization problems have been formulated to estimate an optimal location of the hip cuffs, first to estimate the optimal cuff location at each time step to identify a single 'averaged' optimal cuff location and second to calculate a single optimal cuff location for the entire gait cycle. The optimization solutions identified for the 3DOF model revealed that optimization of the location of cuffs on the anterior and posterior side of the hip joint for 4 cable configuration is not sufficient to generate the desired bi-planar motion. For simultaneous tracking of the bi-planar motion, 2 additional cables have been added at hip joints and are routed in an intra-planar manner. The simulation result with the 3DOF model confirmed successful bi-planar trajectory tracking. The various number of cables and cable routings for tracking bi-planar motion will be studied in future work.

Keywords: cable driven; exoskeleton; lower limb rehabilitation; hip adduction; bi-planar trajectory; optimized routing.

1. Introduction

The literature indicates that a variety of lower-limb robotic devices have been designed in past for stroke rehabilitation, with the majority generating/assisting limb motions by employing a direct actuation approach, such as placing an actuator near the joint to generate joint motion. This design approach, however, induces additional inertia and inertial vibration, assumes knee joints as pin joints, and could induce unnecessary stress and moment/reaction on the knee joint [1] and result in discomfort to the user. This further challenge rehabilitation of the impaired limb due to the addition of extra weight to the already afflicted limb and discomfort to the user. Furthermore, devices designed in past, such as those actuated using pneumatic artificial muscles (PAMS) [2,3], actuated using hydraulic actuators [4], actuated using motors [5–7] actuates combination of ankle-knee-hip (AKH) joint only in the sagittal plane. The lower limb motion has only been modelled in the sagittal plane, and frontal plane motion (hip adduction) has either been ignored or allowed passively in such designs.

Preprints (www.preprints.org) | NOT PEER-REVIEWED | Posted: 26 October 2022 doi:10.20944/preprints202210.0396.v1

Cable driven rehabilitation devices (CDRD) facilitate remote actuation while respecting the biomechanics of the joints. These devices are typical of lighter weight and exert negligible inertia and inertial vibration on the impaired limb. Furthermore, CDRDs do not require exact alignment with the joints, unlike direct actuation-based design, thus reducing donning on/off time and enhancing safety. In the past couple of decades, various CDRD devices were proposed. These include C-ALEX [8,9], ROPES [10], and the two cable-driven exoskeletons suggested by Kirby et al. [11] for the lower limb. Despite many advantages, the majority of these devices provide rehabilitation only in the sagittal plane. ROPES [3] has cable routing in the frontal plane, although, the model was analysed only for the sagittal plane. In our previous work, we proposed C-LREX (Cable Driven Lower Limb Rehabilitation Exoskeleton) [12,13] providing conceptual models with cable routing only in the sagittal plane.

In the majority of lower limb exoskeletons (either for direct or indirect actuation-based devices), the lower limb has been modelled only in the sagittal plane for AKH joint motion. The limitation of restricting the motion to the sagittal plane is usually reasonable since a large amount of the motion impairment lies in the sagittal plane. This assumption, however, is not always justifiable, as hip circumduction in the frontal plane tends to be higher in stroke patients. Previous work on intra-planar cable driven devices can be mainly found for upper limb rehabilitation, including CAREX [14], CAREX-7 [15], and the upper arm cable driven system by Chen et al [16].

This work extends the previous sagittal plane-based model for C-LREX and C-ALEX to accommodate motion in the frontal plane (mainly Hip Adduction/Abduction). Furthermore, we aim to investigate the possibility of intra-planar cable routing at the hip joint to track the bi-planar reference healthy trajectory (sagittal and frontal plane). The first section of the paper layout the lower limb dynamic models for C-LREX as well as trajectory tracking with these models. The next section focuses on the intra-planar routing of hip cables via two different optimization approaches. The effect of different routing on trajectory tracking is studied and a new extended cable routing is proposed. The next section summarizes the model, results of analysis, and limitations followed by a brief conclusion with future work.

2. 3DOF Model

In our previous work [12,13], the models were developed only for the sagittal plane motion (2DOF (degrees of freedom) Model mainly accommodating hip and knee Flexion/Extension) assistance (refer to **Figure 1**(a)). To investigate frontal plane motion and cable routing, the hip joint has been modelled as a two DOF joint (Flexion/Extension and Adduction /Abduction), while the knee joint has been modelled as a single DOF joint (only Flexion/Extension) as depicted in **Figure 1**(b). The internal/external rotation of the hip joint in the transverse plane was neglected in the current model. The model assumes that the foot is fixed to shank perpendicularly (ignore the rotation of the foot) while the inertial properties are used in the model. The model assumes that the user can continue the stance phase of motion on the impaired limb and is thus ignored in the modelling. The model is derived for the swing phase of the motion and is simulated assuming the foot is suspended in the air (mimicking the swing phase).

The dynamic model can be described using Newton Euler's or Lagrange's formulation, where $q=[\phi_1 \quad \theta_1 \quad \theta_2]^T$ is considered as the generalized coordinate, ϕ_1 represents the hip adduction angle, while θ_1 and θ_2 represent the hip and knee flexion angles, respectively. The generalized equation of the dynamics can then be expressed as:

$$M(q)\ddot{q}+C(q,\dot{q})\dot{q}+G(q)=\tau \tag{1}$$

doi:10.20944/preprints202210.0396.v1

Where $M(q)$ is the inertial matrix ($M \in \mathbb{R}^{3\times3}$), $C(q,\dot{q})$ represents the Coriolis component ($C \in \mathbb{R}^{3\times1}$), $G(q)$ represents the Gravitational components ($G \in \mathbb{R}^{3\times1}$), and τ represents the torques on the joints ($\tau \in \mathbb{R}^{3\times1}$).

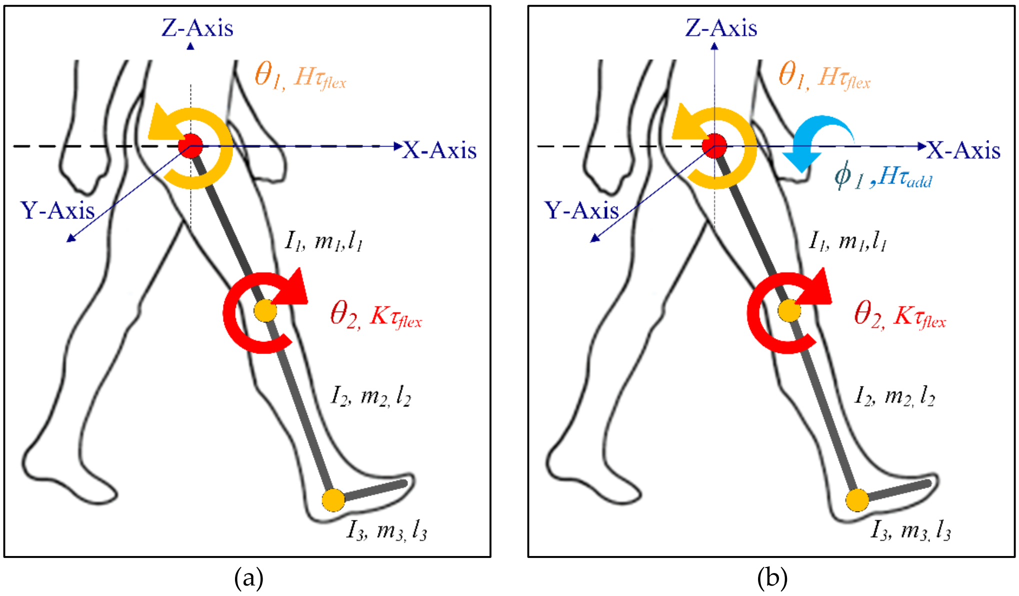

Figure 1. Lower limb model for C-LREX (a) 2DOF (b) 3DOF

The conceptual model with 4 cable configuration is selected to ensure system capability to generate both the positive and negative joint moment independently at each joint (in the sagittal plane) (shown in **Figure 2**) and is referred to as '*planar cuff*' throughout the paper.

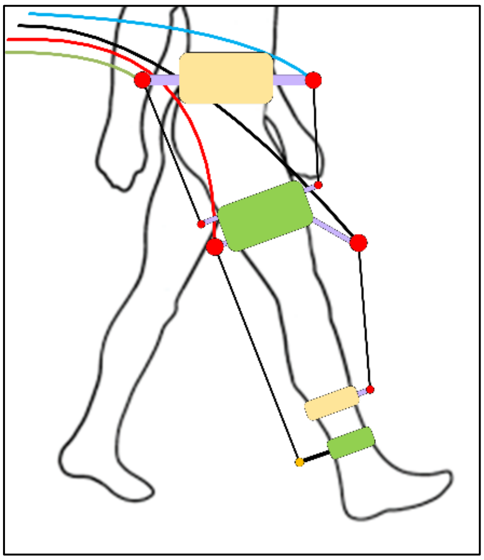

Figure 2. Conceptual model of C-LREX with 4 cables (planar cuff) routing [13]

2.1. Generalized Cuff Definition

The cuff has been defined using 5 parameters (refer to **Figure 3** and **Table 1**), including 2 additional parameters in contrast to the previous 2DOF Model [13]. The sagittal plane cable routing can be transformed into 3D space by setting the additional parameters (fa_lh and ft_lh) to zero. With these parameters, any cuff in 3D space can be fully defined.

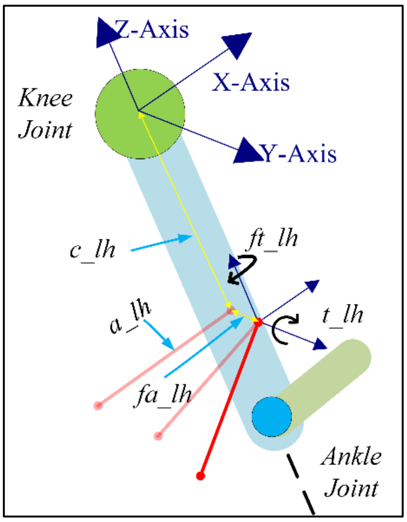

Figure 3. Generalized cuff definition using 5 parameters on Shank

Table 1. Generalized Cuff Parameters Definition

Name	Details
c_lh	Distance of the cuff from the joint center along the Z-axis
a_lh	Distance of the cuff end from the limb central axis along the X-axis
fa_lh	Distance of the cuff base from the limb central axis along the Y-axis
t_lh	Rotation of the cuff about the Y-axis
ft_lh	Rotation of the cuff about the Z-axis

2.2. Force to Joint Torque Mapping

If the cuff locations are known, the relation between cable tension and joint moment can be found [12,13] as:

$$
\begin{gathered}
F = \begin{bmatrix} F_1 & F_2 & F_3 & F_4 \end{bmatrix}^T, \tau = \begin{bmatrix} \tau_1 & \tau_2 & \tau_3 \end{bmatrix}^T \\
B = \begin{bmatrix} J_1 & J_2 & J_3 & J_4 \end{bmatrix}^T = \begin{bmatrix} J_{11} & J_{12} & J_{13} & J_{14} \\ J_{21} & J_{22} & J_{23} & J_{24} \\ J_{31} & J_{32} & J_{33} & J_{34} \end{bmatrix}^T \\
B \in \mathbb{R}^{4\times3}, J \in \mathbb{R}^{3\times1}
\end{gathered}
\tag{2}
$$

The cable tension distribution problem is formulated as a hybrid optimization problem of error minimization (primary) and control effort minimization (secondary), where QP (quadratic programming) is employed for the solution. The hybrid optimization problem solution guarantees the existence of a solution in all possible scenario (particularly when there exist no unique solution in the primary case) [17]. Moreover, a PD controller with the same 3-layer control architecture as the 2DOF model is employed to track the reference healthy trajectory.

The anthropometric data have been adopted from Winter's [18] (based on body weight and height), where the moment of inertia in the frontal plane is considered the same as that in the sagittal plane. The reference trajectory is based on Fukuchi [19] (overground walking of *3.48 s* gait cycle time).

2.3. Trajectory Tracking: Same Cuff Location with the 2 DOF and the 3DOF Models

Both models have been simulated for one gait cycle with the same cuff routing location used in the 2DOF model, with a discrete time step of *0.01 seconds*. The tracking results (shown in **Figure 4**) highlight that the inclusion of the hip adduction degree of freedom

Preprints (www.preprints.org) | NOT PEER-REVIEWED | Posted: 26 October 2022 doi:10.20944/preprints202210.0396.v1

has minimal impact on the trajectory tracking. However, with planar cable routing, the tracking of the hip adduction in the 3 DOF model is similar to the passive hip adduction. This is likely due to planar cable routing which contributes mainly to motion in the sagittal plane.

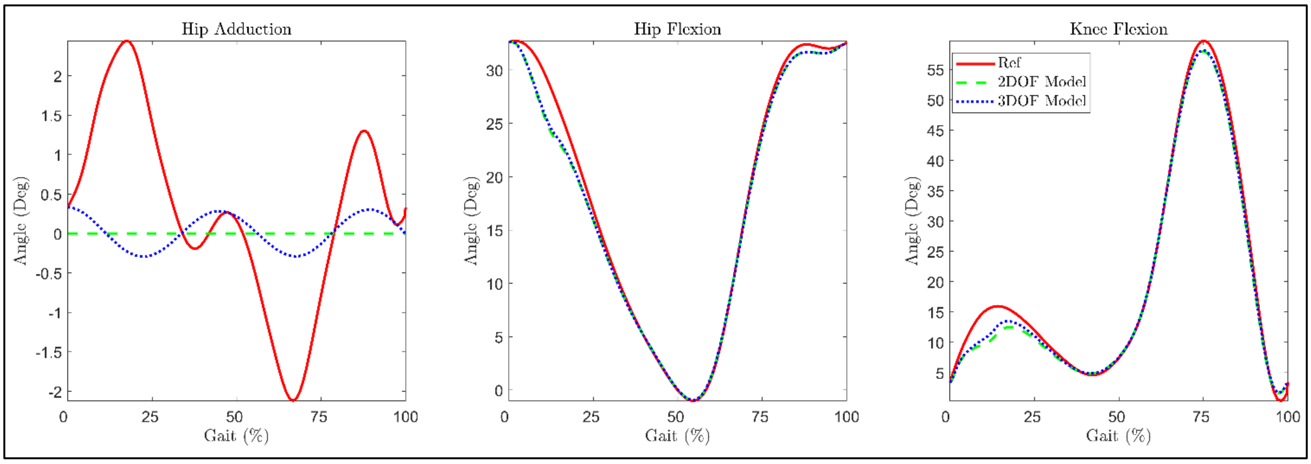

Figure 4. Trajectory tracking with different models employing the same cuff locations

3. Intra-Plane Cable Routing for Hip Adduction

Since the 3DOF model only considers flexion motion for the knee joint, the cable routed for knee motion can be kept the same as the 2DOF model. However, for the hip joint, the moment has to be generated for both sagittal and frontal plane motion, and hence the cable routing has to be modified. The lower cuff of the hip joint is maintained similar to the planar cuff model while the upper cuff location was modified (as shown in **Figure 5**).

To find the suitable location for the upper cuffs (both sides placed on the torso) that can meet the model demand for both sagittal and frontal plane moment demand, we formulated an optimization problem to identify the optimal location of the upper cuff for each timestep of the motion. The optimizer will return an optimized cuff location for each timestep that will meet the joint moment requirement in both the sagittal and frontal planes.

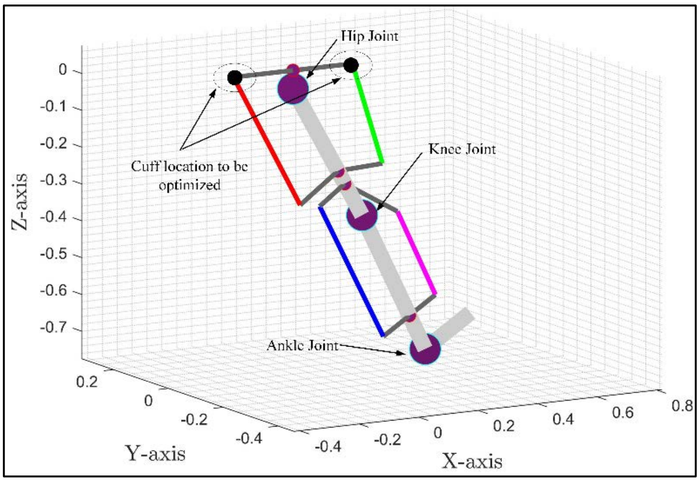

Figure 5. The exoskeleton and the cuff location are to be optimized in 3D space

Since the model needed to optimize the upper cuff location only, the coordinates of the upper cuff have been included as variables. A cuff end location is typically dependent

Preprints (www.preprints.org) | NOT PEER-REVIEWED | Posted: 26 October 2022 doi:10.20944/preprints202210.0396.v1

on 5 variables which can be arranged in multiple ways. To reduce the optimization variables for each cuff from 5 to 3, the cuff end location (*thick black line in* **Figure 6**) is currently being considered along the axes (*red lines in* **Figure 6**), i.e., the angular orientation of the cuff about the axes is fixed.

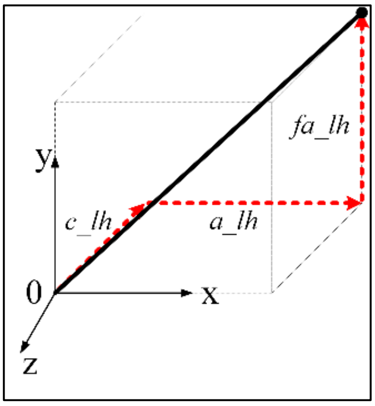

Figure 6. Cuff end location estimation along axes

Assuming $[x_1 \quad y_1 \quad z_1]^T$ and $[x_2 \quad y_2 \quad z_2]^T$ as the positions of the upper cuff on the anterior and posterior sides of the torso, we aimed to minimize the error between the required and generated joint moment such that the cuff position remained within the specified limits and specified cable tension ranges. The optimization problem is then formulated as:

$$\min\left(B^T F - \tau\right)$$
$$s.t. \begin{cases} x_{\min} \le x \le x_{\max} \\ y_{\min} \le y \le y_{\max} \\ z_{\min} \le z \le z_{\max} \\ F_{\min} \le F \le F_{\max} \end{cases} \tag{3}$$

The above static optimization problem will also distribute the cable tension, and thus a separate cable tension distribution problem is not required. The range of values for the variables in the optimization problem is listed in **Table 2**. MATLAB-based *fmincon* function has been employed to solve the above optimization problem.

Table 2. Optimization variable ranges

Variable (Unit)	Min Value	Max Value
x_1 (m)	-0.4	-0.2
y_1 (m)	-0.1	0.1
z_1 (m)	0	0.2
x_2 (m)	0.2	0.4
y_2 (m)	-0.1	0.1
z_2 (m)	0	0.2
F (N)	7	100

The optimal solutions (green and red dots shown in **Figure 7**) are plotted along with the exoskeleton. The trajectory tracking error with the optimized cuff location is shown in **Figure 8**. The maximum error is limited to *1.6 degrees* for knee flexion. The dots pair (**Figure 7**) represents the location of the hip cuff to be situated at a different timestep of motion to track the healthy trajectory closely with the trajectory tracking error shown in **Figure 8**.

Preprints (www.preprints.org) | NOT PEER-REVIEWED | Posted: 26 October 2022 doi:10.20944/preprints202210.0396.v1

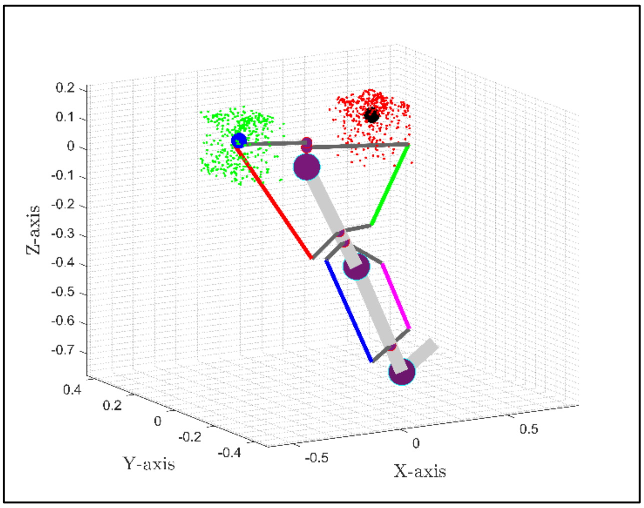

Figure 7. Optimal cuff locations prediction for each cuff (small dots represent optimal location at a different timestep of motion, big dots represent the average of small dots).

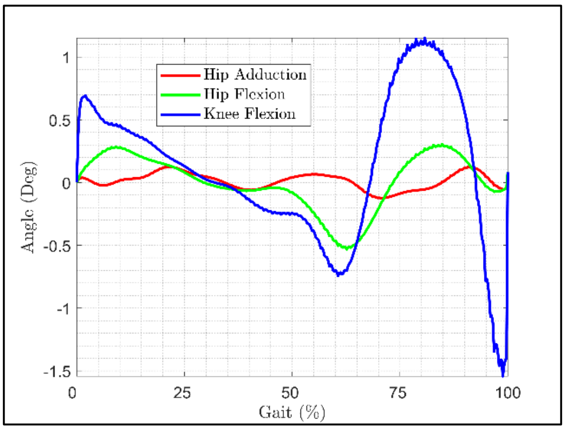

Figure 8. Trajectory tracking error with the optimal cuff at each timestep

Since the current model assumes the cuff positions to be fixed (stationarily attached to a limb or torso), a single point for the cuff location is to be determined. The average of all the optimal points is taken to estimate the single optimal point (shown as a blue and black point in **Figure** 7), referred to as the *'Averaged optimal cuff'*.

A general way to find a single optimal solution for the hinge location would be discretizing the ranges of the coordinate variables, simulating the model for each combination with the same cable tension constraints (7-100 N), and selecting the case where the error in tracking the joint angles is the least. Since this process will require a large amount of time due to the high number of combinations, another optimization problem has been formulated to minimize the error in joint angle tracking as follows:

$$\min\left(e_{hipA}{}^{T}e_{hipA}+e_{hipF}{}^{T}e_{hipF}+e_{kneeF}{}^{T}e_{kneeF}\right)$$
$$s.t.\begin{cases}x_{\min}\le x\le x_{\max}\\ y_{\min}\le y\le y_{\max}\\ z_{\min}\le z\le z_{\max}\end{cases} \tag{4}$$

Where, $e_{hipA}, e_{hipF}, e_{kneeF}$ represent errors in joint angle tracking in hip adduction, hip flexion, and knee flexion respectively. For this optimization case, the cable tension range is excluded from the variable and distributed via quadratic programming.

Preprints (www.preprints.org) | NOT PEER-REVIEWED | Posted: 26 October 2022 doi:10.20944/preprints202210.0396.v1

The above optimization problem converged on the following single optimal solution for the hip cuff locations:

$$\begin{bmatrix} x_1 & y_1 & z_1 & x_2 & y_2 & z_2 \end{bmatrix}^T = X_{opt} = [-0.4 \quad -0.0274 \quad 0 \quad 0.3958 \quad 0.0113 \quad 0]^T$$

3.1. Model Performance with Various Cuff Locations:

The tracking performance of planar, averaged optimal, and single optimal cuff locations are shown in **Figure 9**. With averaged optimal cuff location, the tracking is improved, but, only in the sagittal plane. With the single optimal cuff location, the tracking has been improved both in the sagittal as well as frontal planes. On the other hand, despite the improvement, the frontal plane tracking is not reasonable as the adduction angle is higher in each optimal cuff location than in the planar cuff location. This reflects that each optimal cuff location applies a higher moment in the frontal plane as compared to the planar cuff location. The single optimal cuff location dictates the tracking among others but fails to exert enough moment to track the adduction trajectory closely. Though the tracking in the swing phase (the limb is off the ground during the gait cycle) is similar in each case, the peak cable tension (in optimal cuff locations is reduced as compared to the planar cuff location of the hip cuff, along with improved tracking in the sagittal plane (**Figure 10**).

In general, a single cuff location on the hip on the anterior and posterior side will not be sufficient to generate the desired moment in the frontal plane in addition to the sagittal plane. The 3DOF lower limb model acts as two separate parts attached via the knee joint in the sagittal plane while acts as a single part in the frontal plane (combined lower limb as one part). The intra-planar routing of hip cable results in the generation of cable component forces in both the sagittal and frontal plane, however, in fixed ratio defined by the geometric configuration of C-LREX at the instant of motion. Since the demand of joint moments in sagittal and frontal is in variable ratio during tracking, the intra-planar routing will not be able to track bi-planar trajectory. The current intra-planar cable routing in both optimal cuff location cases results in a dominant component in the sagittal plane than in the frontal plane, and thus trajectory in the sagittal plane is only tracked closely. The tracking failure was observed due to a smaller number of cables, similar to the phenomenon observed in previous work [12] where only one cable was employed to generate hip moment in the sagittal plane in *3_cable_short_configuration* while in the current optimal cuff location-based model, two cables are used to generate bi-planar (two different moments) at the hip joint. This is consistent with the finding that the number of cables must be higher than DOF being constrained for open chain cable driven mechanism [20]. The addition of further intra-planar cables will reduce the dependency to generate intra-planar moments by cables in each plane and may lead to improved bi-planar trajectory tracking.

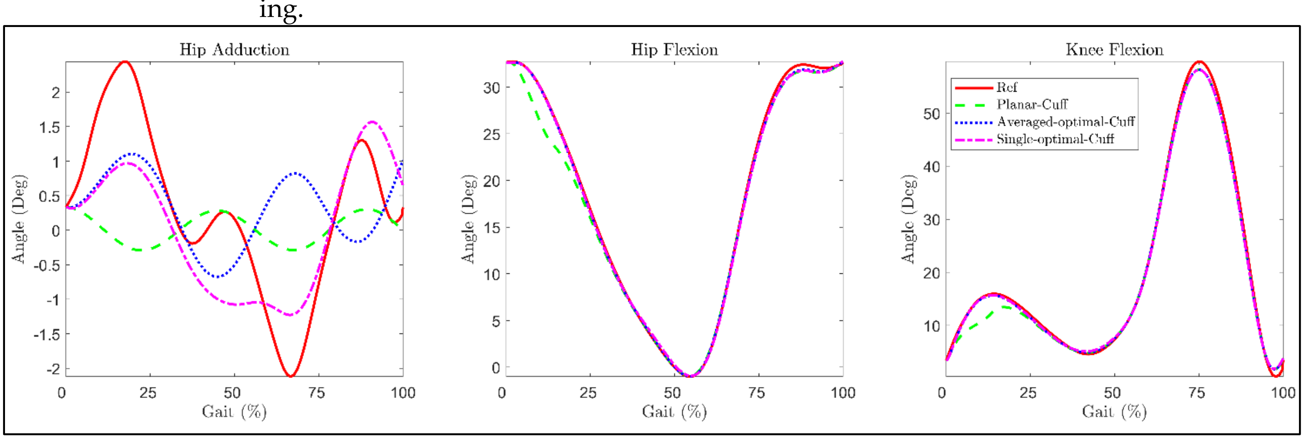

Figure 9. Trajectory tracking with planar cuff location, averaged optimal cuff location, and single optimal cuff location

Preprints (www.preprints.org) | NOT PEER-REVIEWED | Posted: 26 October 2022 doi:10.20944/preprints202210.0396.v1

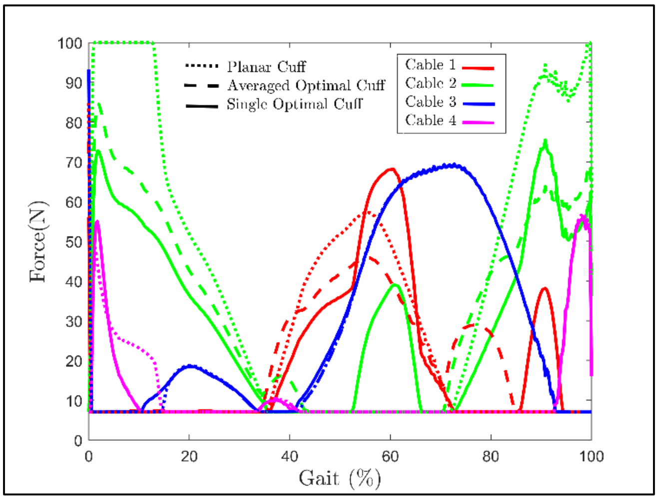

Figure 10. Cable Tension requirements in various cuff locations

3.2. Extended 6 cable exoskeleton model

Despite optimization efforts, it is observed that the 4-cable configuration model fails to meet the trajectory tracking of simultaneous sagittal and frontal plane motion. As a potential solution, two additional cables have been included in the existing 4 cable configuration in the frontal plane (so that bi-directional joint moment can be generated in frontal for hip without leveraging the sagittal plane cables), resulting in an extended 6 cable exoskeleton model (**Figure 11**). The extension enhanced the capability to generate the adduction moment in combination with the flexible moment for hip joint. Unlike in 4 cable configurations with optimal cuff locations in the previous section where the sagittal and frontal joint moments for the hip were generated in a certain relation, the extended 6 cable model can generate a bi-planar moment relatively independent.

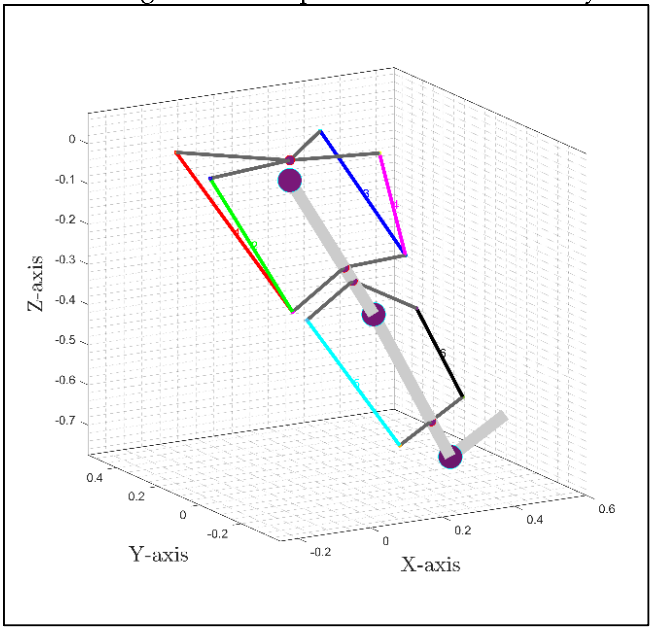

Figure 11. Extended 6 cable configuration (extension of 4 cable configuration)

With the extended configuration, the trajectory tracking, and cable tension requirement is found as shown in **Figure 12** and **Figure 13**. The required cable tensions in model stays below the upper limit with close trajectory tracking.

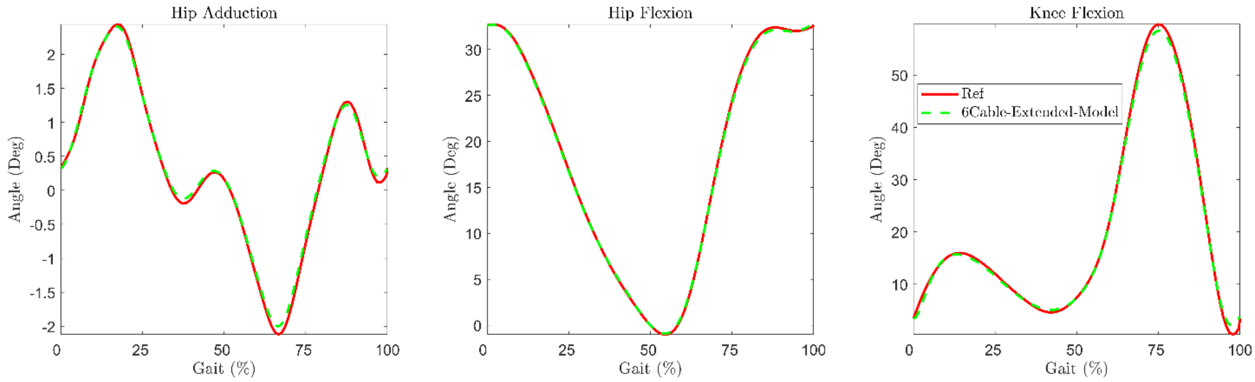

Figure 12. Joint angle tracking for extended configuration

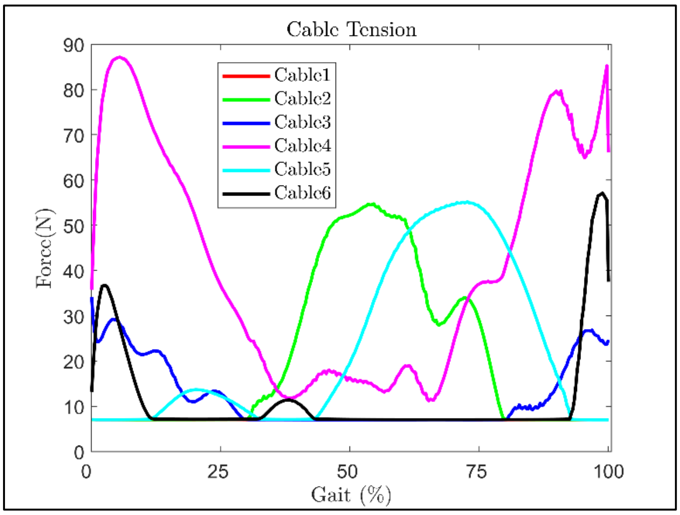

Figure 13. Cable tension distribution requirement in the extended configuration

4. Discussion

The majority of current cable driven exoskeletons used for lower limb rehabilitation operate only in the sagittal plane, hence not addressing movement dysfunction in other planes which are quite common with neurologically induced motion deficit. In this work, we extended 2DOF lower-limb cable driven model to a 3DOF model to accommodate hip adduction motion in the frontal plane. The model assumes the lower limb as a 3-link pendulum model and the limb's inertial and dimensional parameters are estimated via Winter's model based on user height and weight. Alterations in user height and weight will directly influence the user's anthropometric data only with the same model dynamics. It will increases/decrease model joint torque requirements depending on the increase/decrease in inertial parameters. The gait cycle has been adopted from Fukuchi dataset with a slower speed (longer walking time) since the stroke survivors walking speed is reduced compared to healthy. The increase in walking speed will increase the power demands at the joints and vice versa.

The planar cable routing is adapted from previous work (see **Figure 2**) [13], which is mainly routed in the sagittal plane and the cuff location is fixed with respect to the limb section. The simulation of the 3DOF model with planar cable routing revealed that ignoring hip adduction has minimal impact on sagittal plane trajectory tracking provided that the adduction motion is within a small range. In case the adduction motion range is higher, we have investigated the possibility of intra-planar cable routing to track both the sagittal and frontal plane motions simultaneously. The cuffs have been defined using 5 parameters definition for inclusion in the model, however, the axial definition of the cuff endpoint is adopted to reduce the parameters to 3.

Two optimization problems have been formulated to estimate the optimal location of the anterior and posterior cuffs on the torso acting for the hip joint (hip upper cuff) so that both the sagittal and frontal plane moments required can be satisfied. The first optimization problem is formulated to estimate the optimal location at each time step and an average of all the optimal locations has been taken to estimate the 'averaged optimal cuff 'location. Similarly, the second optimization problem estimated a single optimal cuff location for the whole gait cycle. The planar and optimal cuff locations were then considered and simulated with the 3DOF model. The simulation results revealed that a single cable, each on the posterior and anterior side of the hip joint, is not sufficient to generate the desired hip adduction and flexion simultaneously, regardless of employing either planar or optimal cuff locations. The failure in tracking was observed due to an equal number of cables and joint DOF being actively controlled. To track the bi-planar motion, two additional cables have been introduced at the hip level and improve the capability of the system to generate both sagittal and frontal plane moments in both positive and negative directions. The simulation result indicated that the 6-cable configuration can closely track the frontal plane trajectory without sacrificing sagittal plane tracking performance.

5. Conclusions

Due to their simple design, lightweight, remote actuation, and easy safe user interface, Cable driven rehabilitation devices have multiple benefits over traditional link-based devices such as lightweight, provision of remote actuation, and reduced donning on/off time. Due to modelling limitation to the sagittal plane only, CDRDs are failing to address the fontal plane dysfunction. In this work, we have extended the C-LREX 2DOF model to accommodate hip adduction motion (3DOF model).

To investigate the potential of simultaneously tracking bi-planar trajectory, the planar cable routing (4 cable routing) [13]) is modified for hip upper cuff location via two optimization problems, first to estimate optimal cuff location for each timestep and second to estimate a single optimal cuff location. The simulation with the 3DOF model revealed that both planar and optimal cuff location-based routing failed to track desired frontal plane trajectory. Based on the results, we recommend either a variable cuff location-based design or the inclusion of multiple cables to track bi-planar motions simultaneously. An extension of the existing 4 cable configuration to 6 cables, including 2 in the frontal plane is proposed. The preliminary simulation results of the 6-cable scenario indicate that such a configuration can successfully track the trajectories simultaneously in both frontal and sagittal planes. Further solutions exploring the number of cables, routings, and configurations will be addressed in future work.

Author Contributions: Conceptualization, Rajan Prasad and Marwan El-Rich; Funding acquisition, Kinda Khalaf; Methodology, Rajan Prasad; Software, Rajan Prasad; Visualization, Rajan Prasad, Marwan El-Rich, Mohammad Awad, Sunil Agrawal and Kinda Khalaf; Writing – original draft, Rajan Prasad; Writing – review & editing, Mohammad Awad, Sunil Agrawal and Kinda Khalaf. All authors approved the submitted version of the manuscript.

Funding: This publication is based upon work supported by the Khalifa University of Science and Technology under Award RC2-2018-022 (HEIC).

Institutional Review Board Statement: Not applicable.

Data Availability Statement: Data available on request.

Conflict of Interest: The authors declare that the research was conducted in the absence of any commercial or financial relationships that could be construed as a potential conflict of interest.

References

1. Wang, D.; Lee, K.-M.; Guo, J.; Yang, C.-J. Adaptive Knee Joint Exoskeleton Based on Biological Geometries. *IEEE/ASME Trans. Mechatronics* **2014**, *19*, 1268–1278, doi:10.1109/TMECH.2013.2278207.
2. Dao, Q.T.; Yamamoto, S. ichiroh Assist-as-Needed Control of a Robotic Orthosis Actuated by Pneumatic Artificial Muscle for Gait Rehabilitation. *Appl. Sci.* **2018**, *8*, doi:10.3390/app8040499.
3. Koceska, N.; Koceski, S.; Durante, F.; Zobel, P.B.; Raparelli, T. Control Architecture of a 10 DOF Lower Limbs Exoskeleton for Gait Rehabilitation. *Int. J. Adv. Robot. Syst.* **2013**, *10*, 68, doi:10.5772/55032.
4. Glowinski, S.; Obst, M.; Majdanik, S.; Potocka-Banaś, B. Dynamic Model of a Humanoid Exoskeleton of a Lower Limb with Hydraulic Actuators. *Sensors* **2021**, *21*, 3432, doi:10.3390/s21103432.
5. Sanchez-Manchola, M.; Gomez-Vargas, D.; Casas-Bocanegra, D.; Munera, M.; Cifuentes, C.A. Development of a Robotic Lower-Limb Exoskeleton for Gait Rehabilitation: AGoRA Exoskeleton. In Proceedings of the 2018 IEEE ANDESCON; IEEE, August 2018; pp. 1–6.
6. Wu, J.; Gao, J.; Song, R.; Li, R.; Li, Y.; Jiang, L. The Design and Control of a 3DOF Lower Limb Rehabilitation Robot. *Mechatronics* **2016**, *33*, 13–22, doi:10.1016/j.mechatronics.2015.11.010.
7. Unluhisarcikli, O.; Pietrusinski, M.; Weinberg, B.; Bonato, P.; Mavroidis, C. Design and Control of a Robotic Lower Extremity Exoskeleton for Gait Rehabilitation. In Proceedings of the 2011 IEEE/RSJ International Conference on Intelligent Robots and Systems; IEEE, September 2011; pp. 4893–4898.
8. Jin, X.; Cui, X.; Agrawal, S.K. Design of a Cable-Driven Active Leg Exoskeleton (C-ALEX) and Gait Training Experiments with Human Subjects. In Proceedings of the 2015 IEEE International Conference on Robotics and Automation (ICRA); IEEE, May 2015; Vol. 2015-June, pp. 5578–5583.
9. Jin, X.; Prado, A.; Agrawal, S.K. Retraining of Human Gait - Are Lightweight Cable-Driven Leg Exoskeleton Designs Effective? *IEEE Trans. Neural Syst. Rehabil. Eng.* **2018**, *26*, 847–855, doi:10.1109/TNSRE.2018.2815656.
10. Alamdari, A.; Krovi, V. Design and Analysis of a Cable-Driven Articulated Rehabilitation System for Gait Training. *J. Mech. Robot.* **2016**, *8*, doi:10.1115/1.4032274.
11. Witte, K.A.; Fatschel, A.M.; Collins, S.H. Design of a Lightweight, Tethered, Torque-Controlled Knee Exoskeleton. In Proceedings of the 2017 International Conference on Rehabilitation Robotics (ICORR); IEEE, July 2017; pp. 1646–1653.
12. Prasad, R.; Khalaf, K.; Awad, M.I.; Hussian, I.; Jelinek, H.F.; Huzaifa, U.; Rich, M. El A Generalized Framework for the Assessment of Various Configurations of Cable-Driven Mobile Lower Limb Rehabilitation Exoskeletons. In Proceedings of the 2022 12th International Conference on Biomedical Engineering and Technology (ICBET); ACM: New York, NY, USA, April 20 2022; pp. 133–140.
13. Prasad, R.; El-Rich, M.; Awad, M.I.; Hussain, I.; Jelinek, H.F.; Huzaifa, U.; Khalaf, K. A Framework for Determining the Performance and Requirements of Cable-Driven Mobile Lower Limb Rehabilitation Exoskeletons. *Front. Bioeng. Biotechnol.* **2022**, *10*, doi:10.3389/fbioe.2022.920462.
14. Mao, Y.; Agrawal, S.K. Design of a Cable-Driven Arm Exoskeleton (CAREX) for Neural Rehabilitation. *IEEE Trans. Robot.* **2012**, *28*, 922–931, doi:10.1109/TRO.2012.2189496.
15. Cui, X.; Chen, W.; Jin, X.; Agrawal, S.K.; Member, S. Design of a 7-DOF Cable-Driven Arm Exoskeleton (CAREX-7) and a Controller for Dexterous Motion Training or Assistance. **2017**, *22*, 161–172, doi:10.1109/TMECH.2016.2618888.
16. Chen, W.; Li, Z.; Cui, X.; Zhang, J.; Bai, S. Mechanical Design and Kinematic Modeling of a Cable-Driven Arm Exoskeleton Incorporating Inaccurate Human Limb Anthropomorphic Parameters. *Sensors* **2019**, *19*, 4461, doi:10.3390/s19204461.
17. Prasad, R.; Ma, Y.; Wang, Y.; Zhang, H. Hierarchical Coordinated Control Distribution and Experimental Verification for Six-Wheeled Unmanned Ground Vehicles. *Proc. Inst. Mech. Eng. Part D J. Automob. Eng.* **2020**, 095440702094082, doi:10.1177/0954407020940823.

 doi:10.20944/preprints202210.0396.v1

18. Winter, D.A. *Biomechanics and Motor Control of Human Movement*; John Wiley & Sons, Inc.: Hoboken, NJ, USA, 2009; Vol. 2nd; ISBN 9780470549148.
19. Fukuchi, C.A.; Fukuchi, R.K.; Duarte, M. A Public Dataset of Overground and Treadmill Walking Kinematics and Kinetics in Healthy Individuals. *PeerJ* **2018**, *6*, e4640, doi:10.7717/peerj.4640.
20. Mustafa, S.K.; Agrawal, S.K. On the Force-Closure Analysis of n-DOF Cable-Driven Open Chains Based on Reciprocal Screw Theory. *IEEE Trans. Robot.* **2012**, *28*, 22–31, doi:10.1109/TRO.2011.2168170.